Exploring impacts of deployment sequences of industrial mitigation measures on their combined CO_2 reduction potential

de Raad, Brendon; van Lieshout, Marit; Stougie, Lydia; Ramirez, Andrea

DOI
10.1016/j.energy.2022.125406

Publication date
2023

Document Version
Final published version

Published in
Energy

Citation (APA)
de Raad, B., van Lieshout, M., Stougie, L., & Ramirez, A. (2023). Exploring impacts of deployment sequences of industrial mitigation measures on their combined CO_2 reduction potential. *Energy*, *262*, Article 125406. https://doi.org/10.1016/j.energy.2022.125406

Important note
To cite this publication, please use the final published version (if applicable).
Please check the document version above.

Energy 262 (2023) 125406

Contents lists available at ScienceDirect

Energy

journal homepage: www.elsevier.com/locate/energy

Exploring impacts of deployment sequences of industrial mitigation measures on their combined CO_2 reduction potential

Brendon de Raad [a,b,*], Marit van Lieshout [a], Lydia Stougie [b], Andrea Ramirez [b]

[a] Knowledge Centre Sustainable Port Cities, Rotterdam University of Applied Sciences, the Netherlands
[b] Department of Engineering Systems and Services, Delft University of Technology, Delft, the Netherlands

1. Introduction

The industrial sector has to halve its CO_2 emissions by 2030 to mitigate human-induced climate change [1,2]. Decarbonizing heat sources and implementing energy efficiency measures have the potential to reduce the sector's overall CO_2 emissions by 80% [2]. Several studies have explored the reduction potential of individual measures. For instance, Yáñez et al. [3] calculated the expected CO_2 reduction potential of twenty energy efficiency measures in the Colombian oil industry. Similarly, Hasanbeigi et al. [4] identified twenty-three energy efficiency improvements for the Chinese cement industry. In these studies, the combined CO_2 reduction potential is the sum of the potential of the individual measures. The impact of plausible interactions between these measures is assumed to be covered by taking conservative estimates and working with ballpark estimates [3,5]. However, these methods may be insufficient, as interactions between measures could have a severe impact [6].

A portfolio of mitigation measures is commonly not deployed simultaneously due to, among others, limited resources [7]. The sequencing of these measures is often based on a Marginal Abatement Cost Curve (MACC), which is a well-known approach for evaluating and identifying cost-effective options [8–11]. However, this approach has some limitations. For instance, it does not consider the effects of temporal dynamics and interactions between measures [12]. As a result, incremental CO_2 reductions by a new measure might be (partially) negated. Berghout et al. [13] worked around these limitations by adding a bottom-up analysis and studied interactions between short and medium-term mitigation measures. The authors report no significant interactions between energy efficiency measures and other CO_2 reduction measures. Wiertzema et al. [14], however, found strong CO_2 emission reduction trade-offs when focusing on a specific set of energy efficiency measures, namely heat integration measures.

One heat integration measure that is increasingly gaining interest in the industrial sector is a heat pump [15,16]. This emerging high-potential waste heat technology is often among the most cost-competitive CO_2 reduction technologies and is therefore likely to be among the first to be deployed [17]. However, the performance of a heat pump is defined by the processes it is connected to and these conditions may change with the deployment of other CO_2 reduction measures [18]. Therefore, a stand-alone assessment of heat pumps is likely to give an unjust representation of its contribution to the combined CO_2 reduction potential.

This research examines how the deployment sequence of mitigation measures affects their combined CO_2 reduction potential in a biodiesel plant. The emphasis is on the interaction between heat integration measures, energy efficiency measures, and measures that decarbonize heat sources. A better understanding of the impact of the deployment sequence is needed to make more realistic estimates of the combined CO_2 reduction potential in the industrial sector, to identify effective deployment sequences of CO_2 mitigation measures, and to avoid lock-ins that prevent further decarbonization.

2. Method

The impact of process changes on the performance of heat integration measures, such as heat pumps, was assessed by studying future plant layouts. The approach consists of three steps: 1. exploration of future plant layouts, 2. assessment of heat pump opportunities, and 3. analysis of deployment sequences.

2.1. Exploration of future plant layouts

Interactions between different types of mitigation measures were explored by dividing the plant into a reaction section, a separation section, a waste heat recovery section, and a power section (Fig. 1) [19]. CO_2 mitigation measures were identified for each section based on a literature review.

In light of the approaching 2030 reduction target, CO_2 mitigation

* Corresponding author. Knowledge Centre Sustainable Port Cities, Rotterdam University of Applied Sciences, the Netherlands.
E-mail addresses: B.W.de.Raad@HR.nl (B. de Raad), M.van.Lieshout@hr.nl (M. van Lieshout), L.Stougie@tudelft.nl (L. Stougie), C.A.RamirezRamirez@tudelft.nl (A. Ramirez).

https://doi.org/10.1016/j.energy.2022.125406
Received 2 April 2022; Received in revised form 28 July 2022; Accepted 6 September 2022
Available online 9 September 2022

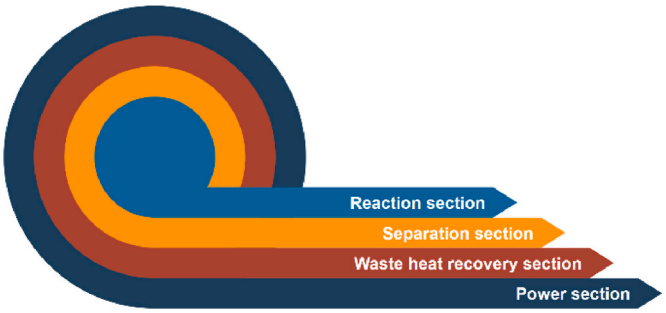

Fig. 1. Onion diagram by Douglas [22] adapted to divide production plants into connected sections.

measures with a Technology Readiness Level of at least 7 were considered.

The resulting list of CO_2 mitigation technologies was qualitatively ranked per process section. The ranking was based on the expected energy savings. A minus symbol (−) indicates an expected increase in heating requirements, a zero (0) was assigned when no significant changes are expected, while a plus symbol (+) reflects a decrease in heating requirements. The number of symbols represents the relative impact of the expected changes. The technologies with the highest individual positive impact per section were selected for the assessment of heat pump opportunities. The resulting layouts enabled the assessment of the sole deployment of each technology, the combination of process improvements, the combination of each technology with a heat pump, and a combination of process improvements with a heat pump.

2.2. Assessment of heat pump opportunities

The heat pump is placed across the pinch point to effectively reduce net heating requirements [20,21]. The pinch point was identified with the help of pinch analysis [22,23]. In this assessment, the heat pump was coupled to the hot (in surplus of heat), and cold (in demand of heat) streams closest to the pinch, with a thermal duty of at least 10% of the total heating requirements. These streams were identified by using the software named PinchAnalysis [24]. Here, the thermal requirements of the main streams (top 90%) of the process were used as input. The specific heat of the media in these streams was assumed to be constant, as the operational data showed no deviation larger than 10%. Heat integration was limited with a minimal temperature difference of 10 °C [23]. The minimal temperature driving force for the heat pump was

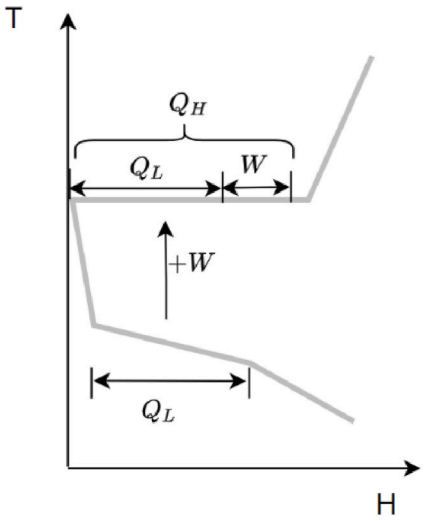

Fig. 2. Integration of a single source heat pump in a grand composite curve -.

neglected. Grand composite curves (GCC) were used to size the heat pump, as in Fig. 2 [20,22,25]. The heat from a cold reservoir (Q_L) is pumped to the temperature level of the high-temperature sink, where at this high-temperature heat (Q_H) is transferred to the hot sink. Q_H is the sum of Q_L and the work (W) added by the heat pump.

The performance of the heat pump was expressed in the Coefficient of Performance (COP), which is calculated with $COP = Q_h/W$. For an ideal (Carnot) heat pump, this simplifies to $T_H/(T_H - T_L)$, where T_H is the temperature of the heat sink and $(T_H - T_L)$ the required temperature lift by the heat pump. An efficiency factor (μ) is required to calculate the non-ideal COP. A factor of 0.55 is used in this assessment, which is common for a mechanical heat pump [26,27].

2.3. Analysis of deployment sequence

All sequence variations of process changes that affect the heat integration potential are explored based on the results of the two previous steps and the conversion of heat and electricity consumption to CO_2 emissions. Process changes that did not affect the heat integration potential were exempted from this analysis for clarity of results. Emissions from heat consumption were based on a well-to-wheel emission factor of natural gas of 56.4 kg/GJ and a gas-fired boiler efficiency of 95% [28,29]. The emissions related to electricity generation were calculated based on the expected well-to-wheel CO_2 emissions of the Dutch electricity grid, which averages at 0.569 kg/kWh between 2020 and 2029 [30]. Yearly operating hours were taken at 8760.

3. Plausible future layouts of a biodiesel production plant

The biodiesel production plant was selected as a case study because it represents a typical production plant in the industrial sector with moderate operational temperatures, CO_2 emissions strongly linked to heating requirements, and a relatively simple plant layout.

3.1. Process description

The most common route to produce low-carbon biodiesel is by converting oil triglycerides into fatty acid methyl esters (FAME) [31]. This conversion is commonly enabled by transesterification with methanol (molar ratio 5.5:1) and a homogeneous base catalyst (~1 wt% NaOH) [32]. For this process, a plant design is available from Air Liquide, as presented in Fig. 3 [32,33]. This plant layout was used as the reference case. The process starts with removing gums, phosphatides, and soaps from the crude oil in a reactor at 45 °C. Hereafter, the degummed oil is deacidified in a distillation column operating at about 240 °C. The neutralized oil is added to two cascaded continuously stirred reactors with two sedimentation tanks operating at temperatures between 50 °C and 60 °C (separators 1 and 2 in Fig. 3). Here, FAME and glycerol, are separated. After a second sedimentation tank, by-products are neutralized and the FAME (<5 wt% water) is washed off. After washing, the FAME is dried to the required product quality. The excess methanol together with the washing water and contaminants are added to the glycerol-methanol mixture from the bottom of the sedimentation tanks. Methanol is recovered from this combined tank in a distillation column with a reboiler temperature of 110 °C. From the top stream, nearly pure methanol is extracted at a temperature of about 60 °C. This stream is combined with fresh methanol and catalyst before re-entering the reactor. The bottom stream, mainly glycerol and water, is dried in a series of drying columns until reaching the required product quality. The evaporated water is reused in the washing tower [31,32,34].

3.2. Exploration of future plant layouts

Possible CO_2 mitigation technologies for the biodiesel production plant with a TRL of at least 7 that could be placed alongside the heat pump in the heat recovery section are summarized in Table 1. The

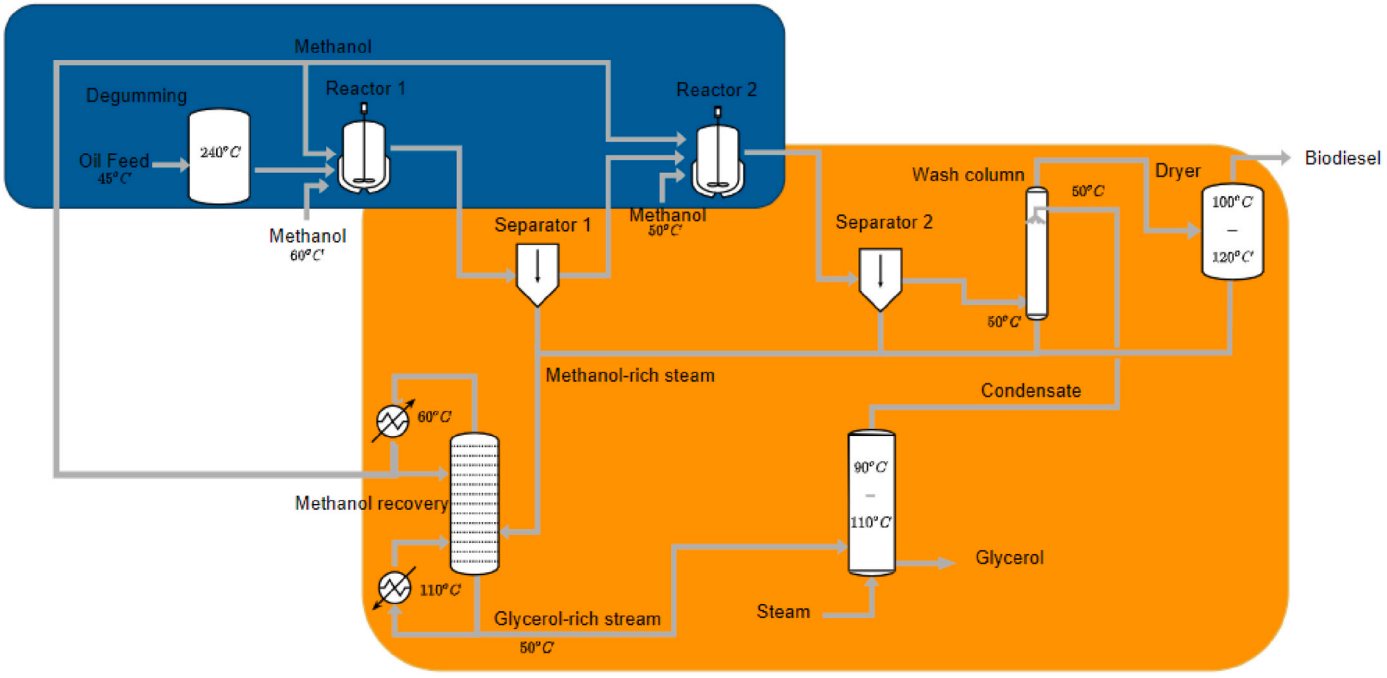

Fig. 3. Plant layout of the reference case (L1) based on the Air Liquide design [32]. The top-left area is defined as the reactor section and the bottom right area is the separation section.

Table 1
Considered technologies for each section of the biodiesel production plant and their expected energy savings per section-

Sections	Technology	Expected effects on heating requirements	Expected overall reduction in heating requirements	TRL	Reference
Reaction	Homogeneous sour catalyst instead of the current homogeneous base catalyst.	(+) there is no production of soap which results in a slightly higher conversion rate (–) Requires higher methanol: oil ratio by a factor of 5, thereby increasing heating requirements (–) operational temperature increases from 58 °C to 110 °C, which is above the pinch and thus increases overall heat demand	–	8–9	[35–38]
	Heterogeneous catalyst basic instead of the current homogeneous base catalyst.	(+) catalyst (solid) separation via filtration, reduces the amount of water required for washing (–) Increased methanol: oil ratio by a factor of 3, thereby increasing heating requirements	–	8–9	[39,40]
	Heterogeneous catalyst sour instead of the current homogeneous base catalyst.	(+) catalyst (solid) separation via filtration, this reduced the required amount of water for washing (–) Increased methanol: oil ratio by a factor of 3, thereby increasing heating requirements (–) the operational temperature increases to 110 °C, which is above the pinch and thus increases overall heat demand	–	8–9	[40,41]
	membrane reactor with methanol-recycling instead of the ambient pressure CSTR.	(+) higher conversion rate (about 3%), lower specific heat consumption (+) purer downstream products, therefore, requiring less separation (++) about 75% less methanol of the methanol-rich stream must be recovered as it can be recycled	++	7–8	[42–44]
Separation	Membrane separation unit instead of sedimentation tanks.	(0) Speed up separation, but as sedimentation has no heating requirement, there are no impacts on the heat balance	0	7–9	[45]
	Membrane separation unit instead of the water washer.	(+) Requires no water from water washing thereby avoiding drying requirements (expected reduction 100% reduction of local heating requirements, about 5% of total heating requirement)	+	7–9	[36, 46–50]
	Divided wall column to replace the methanol recovery and glycerol drying column.	(++) Integration of methanol and glycerol recovery reduces reboiler loads (expected reduction of 30% of local heating requirements, about 20% of total heating requirement)	++	8–9	[51–53]
Power	The use of low carbon fuels in the current natural gas boiler.	(–) increased heating requirements above the pinch for reforming and separation processes	–	9	[54,55]
	E-boiler instead of the gas-fired boiler.	(+) lack of primary energy being lost to flue gasses increases overall heat requirement by about 5%	+	9	[56]
	Feed the current boiler with recycled process gas from the anaerobe water cleaning.	(+) reduced need for natural gas (1% of total heating requirements) (–) increased heating demand due to the need for scrubbing	0	9	[57]

following technologies were selected based on the reduction in expected heating requirement per section (fourth column of Table 1):

1. a membrane reactor with methanol-recycling as an alternative technology for the reactor section,
2. a divided wall column for the glycerol stream for the separation section,
3. an e-boiler for the power section.

The basis for the overall assessment was an energy and mass balance of the main streams of the biodiesel production plant (layout 1). The presence of unreacted products and other contaminants, like free fatty oils, were omitted. The resulting model was calibrated using industrial process data. Layout 2 is the layout that results after deployment of the heat pump in layout 1.

3.2.1. Plant layouts 3 and 4: modifications in the power section

The natural gas-fired boiler was replaced by an e-boiler in layout 3. The process flow diagram of this layout is the same as the reference case (Fig. 3.) since no heat from the flue gas section is directly transferred to the production process. Hence, the energy and mass balances of the first layout remained unchanged from the reference case, just as the heat integration potential. The addition of a heat pump results in layout 4.

3.2.2. Plant layout s 5 and 6: modifications in the separation section

The methanol-recovery column and the glycerol-drying column of the reference case were replaced by a divided wall column in layout 5, which separates the column feed into three nearly pure streams, namely: methanol at the top, water in the middle, and crude glycerol at the bottom (Fig. 4). This column was based on a design by Kiss et al. [42,52,53], and operates at a pressure of 0.5 bar, with a reflux ratio of 0.83 and a feed stream temperature of 60 °C. The concentrations of the feed were taken from the process data. The thermal duty of the condenser was estimated based on the reflux rate (RR), the heat of evaporation (Δh_{evap}), and the methanol distillate rate ($\varphi_{m,d}$) using equation (1).

$$Q_{cond} = (1 + RR) \cdot \Delta h_{evap} \cdot \varphi_{m,d} \tag{1}$$

The requirements for evaporating the water fraction (equation (1) with a reflux rate of zero) and preheating the glycerol and water fraction were considered to determine the duty of the reboiler. The amount of energy required for preheating was calculated with equation (2), where the required duty to heat the species ($\dot{Q}$) is the product of the mass flow ($\dot{m}$), the specific heat of the species (c_p) and the temperature difference (ΔT). The average operating temperature was based on the model by Kiss and Ignar at 105 °C [53]. After the condenser, methanol is at the appropriate temperature to be sent back into the reactor. The water stream was condensed and cooled back to 50 °C before entering the washing column. The glycerol was cooled down to a temperature of 30 °C. The available heat in these coolers and condensers was calculated using equations (1) and (2). Note that as the glycerol and water leave the column in separate steams, the glycerol drying step needed in layout 1 could be omitted. The addition of a heat pump makes for layout 6.

$$\dot{Q} = \dot{m} \cdot c_p \cdot \Delta T \tag{2}$$

3.2.3. Plant layouts 7 and 8: modifications to the reactor section

A membrane reactor with methanol-recirculation is used for the transesterification process in layout 7. The reactor design is based on the work by Cao et al. [42] and operates at 65 °C. The reactors, post reactor coolers, and their separation tanks were omitted. The resulting process flow diagram is presented in Fig. 5. The increase in conversion efficiency of about 2% is expected to have a negligible effect on the energy and mass balances [36,43]. After the reactor, the product is cooled down to 15 °C and separated in a sedimentation tank. The available heat in the cooler was calculated with equation (2), assuming a specific heat capacity of the mixture of 2.13 kJ/kg K. The upper, FAME-rich stream, consists only of FAME and methanol (molar ratio of 10:1), which is comparable with the current flow composition [42]. The FAME-rich phase is brought to market specifications by washing and drying. The design of the wash column was left unchanged, as the concentration of methanol in the stream is comparable with the reference case. The methanol and water used in this process are fed in the methanol-recovery column. Only 75 wt% of the total methanol-rich (>70 wt% methanol) phase was recycled into the reactor to limit the accumulation of glycerol [42]. Before entering the reactor, this stream was brought back to the reaction temperature. This heating requirement was calculated using equation (2). The remaining 25% of the methanol-rich stream is mixed with the waste products of the FAME purification process and led to the methanol-recovery column. The

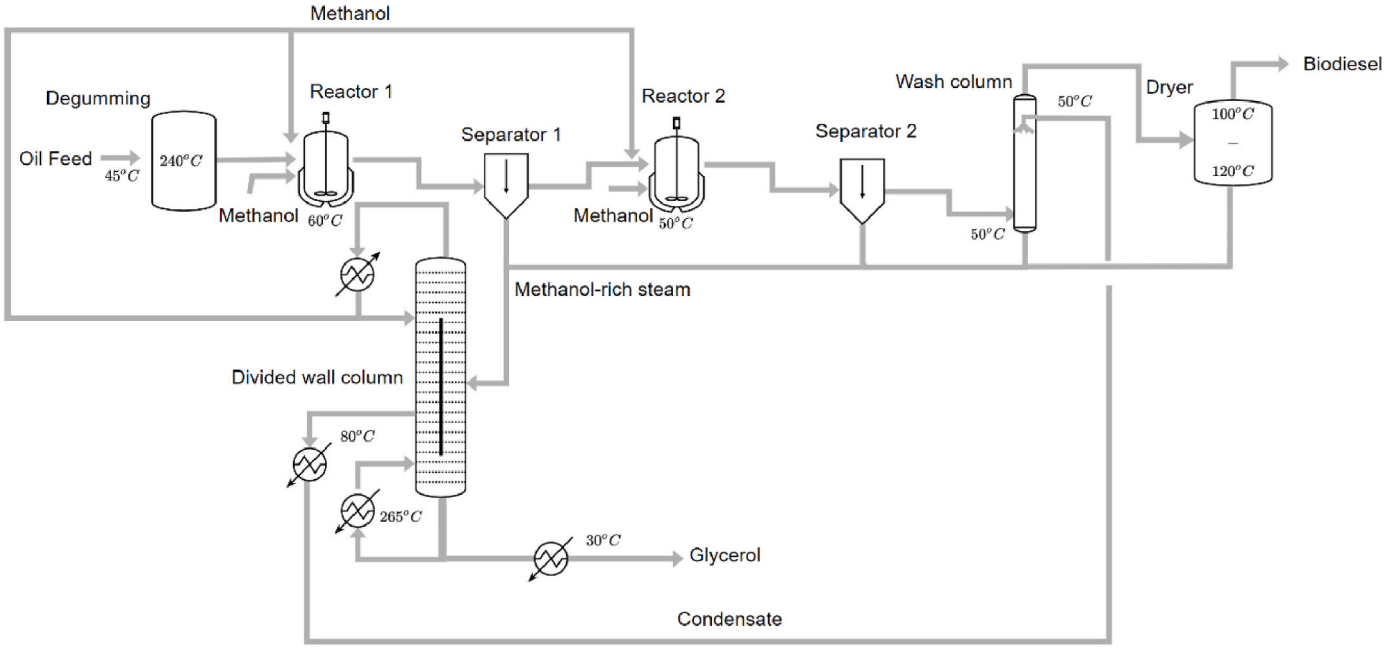

Fig. 4. Plant layout of the plant with a divided wall column (L5).

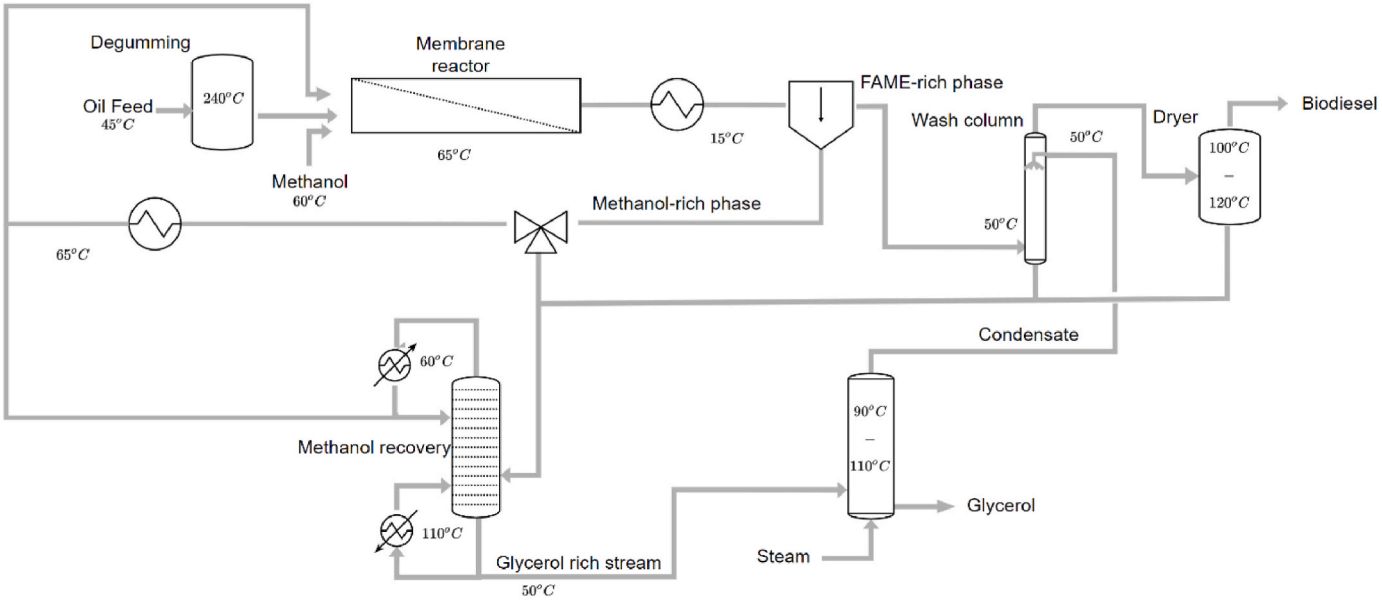

Fig. 5. Plant layout of the plant with a membrane reactor (L7).

recycling of methanol results in a lower flux of methanol compared to the reference case. Therefore, the reboiler and condenser of this layout were redesigned based on equation (1) but using the same reflux rate as in the reference case, i.e., 1.2. The reboiler duty was estimated as the sum of the condenser duty and the required heat for preheating (equation (2)). The addition of a heat pump makes for layout 8.

3.2.4. Plant layouts 9 and 10: modifications to the separation and reactor section

In this layout, a membrane reactor was introduced together with a divided wall column. The resulting process flow diagram is depicted in Fig. 6. Here, the process units were modelled in the same way as in the plant layouts 5 and 7. The addition of a heat pump makes for layout 10.

4. Results

Interactions between the process changes are elucidated by first covering the impacts individual and combined measures had on the heat integration potential of the biodiesel production site in section 4.1. Section 4.2 explores the impact of the deployment sequence on the combined CO 2 reduction potential.

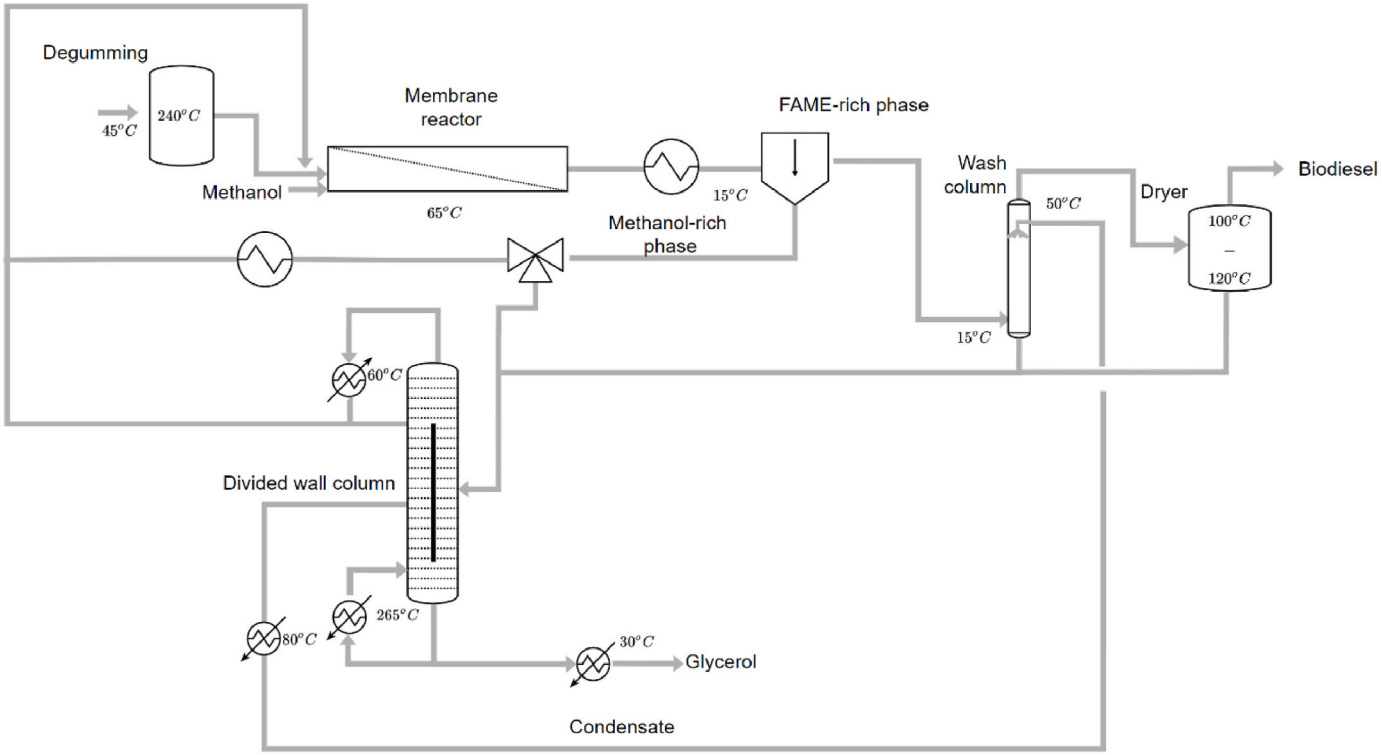

Fig. 6. Plant layout of the plant with a divided wall column and a membrane reactor (L9).

4.1. Assessment of heat pump opportunities

The grand composite curves (GCCs) of all layouts discussed in chapter 3 are depicted in Fig. 7 A-H. These graphs show the changes in thermal requirements resulting from deploying the CO_2 mitigation measures. From Fig. 7A, it can be derived that 2.4 MW of heat was required to operate the current plant layout (L1). The highest temperatures were required by the deacidification process of the crude oil before it entered the reactor at about 250 °C. Nevertheless, most heat (1.9 MW) was required around 110 °C to evaporate the methanol in the reboiler of the methanol-recovery column. The pinch was formed at about 100 °C by the FAME drying process. This pinch extends to a near pinch at about 60 °C, where the condensation heat of the methanol (1.4 MW) from the same recovery column became available. The reboiler and condenser of this column were taken as the sink and source for a heat pump. Their location in the T-H diagram is indicated by the dotted line. The effect of connecting these streams with this heat pump is depicted in Fig. 8B (L2). Connecting these streams required 0.4 MW. The GCC of Layout 2 (L2) shows that another heat pump could save an additional 0.25 MW. The GCC also holds for layouts 3 and 4, where the e-boiler replaced a natural gas-fired boiler.

The deployment of the divided wall column reduced heating requirements to 1.8 MW in layout 5 (Fig. 7C). This reduction aligns with the expected savings reported by Kiss et al. of 20–30% [51]. Most heat (1.6 MW) was required at a temperature of about 260 °C in the reboiler of the column set by the evaporation temperature of glycerol at 0.5 bara. The GGC shows a near pinch at 240 °C, where heat was required for the deacidification process. This near pinch extends via a pocket until the actual pinch temperature of about 100 °C is formed by the FAME drying process. The water condenser, 0.2 MW at about 75 °C, and the methanol condenser 1.3 MW at about 50 °C of the divided wall column were the most noticeable cooling loads below the pinch. The total cooling requirements, in this layout, were larger than those in the reference layout as exit streams were modelled to be cooled to environmental conditions. Due to the relative size and the location near the pinch, both the reboiler and the condenser of the divided wall column were potential sinks and sources for the heat pump. Nonetheless, as the temperature of the reboiler exceeded the operational range of current heat pump technologies (condenser temperatures of over 250 °C and a temperature lift of about 200 °C [58–60]), this case had no feasible heat pump solution. Neither were there other significant heat sinks to which a heat pump could be connected. Hence, layout 6 was declared infeasible (Fig. 7D).

The deployment of the membrane reactor reduced the heating requirement to 1.9 MW in layout 7 (Fig. 7E). This reduction is due to the reduced mass flow through the methanol-recovery column, whose reboiler duty was reduced to 1.5 MW. The effect is however limited, as most of the methanol stream originated from the wash column and the FAME dryer. These streams were contaminated with water, so they could not be recycled and had to be directly fed to the recovery column. The pinch temperature was again formed by the FAME dryers at about 100 °C and most cooling requirements were from the column's condenser (1.1 MW). The heat pump of layout 8 transferred heat from the column's condenser to its reboiler and reduced heating requirements to 0.5 MW, whilst it required 0.4 MW (Fig. 7F).

The introduction of both the membrane reactor and the divided wall column in layout 9 reduced heating requirements to 1.7 MW (Fig. 8G). Most of the heat was required in the reboiler of the divided wall column to 260 °C. This duty was reduced to 1.3 MW by recycling the methanol-rich stream. The largest cooling requirements stemmed from the divided wall columns methanol and water condensers, at 1.1 MW and 0.2 MW, respectively. The heat integration pocket that was formed in Layout 5 is negated by the introduction of the membrane reactor. As a result, a small heat pump could be installed to future reduce heating requirements to 1.5 MW in layout 10 (Fig. 7H). About 0.1 MW is needed to operate the heat pump. The pinch temperature is again around 100 °C, showing pinch-stability for all layouts, though the adjacent heat sinks and sources change in temperature.

4.2. Analysis of the deployment sequence

The energy consumption and the yearly CO_2 emissions of the ten layouts are presented in Table 2 and visualized in Fig. 8. They show that the deepest cuts in total emissions, from 4.6 to 2.5 kt/a, are achieved when the deployment starts with the membrane reactor, followed by the divided wall column and thereafter the heat pump. The deployment of an e-boiler should be avoided with the assumed carbon intensity as it increases heating emissions by a factor of 2.7. The deployment sequence should also preferably start with a membrane reactor when only emissions from natural gas combustion are accounted for. The sequence should continue with the deployment of a heat pump and end with an e-boiler to fully avoid emissions from natural gas combustion. Inverting the deployment sequence would likely result in the same reduction with an over-dimensioned heat pump and e-boiler. A sole e-boiler would be able to achieve the same results at the cost of high CO_2 emissions from electricity generation.

The membrane reactor (MR), the divided wall column (DWC), and the heat pump (HP) are used to build the six deployment sequences presented in Fig. 8, as they affect the heat integration potential of the production plant. The e-boiler is excluded as it does not. Each of the deployment sequences of Fig. 8 starts with the 4.6 kt/a of CO_2 emissions caused by using natural gas in the reference layout (L1). Fig. 8A shows that emissions from natural gas are cut by 3.5 kt/a to a value of 1.1 kt/a when a heat pump is deployed. However, a large part of this reduction is counterbalanced by an increase in emissions from electricity generation, which makes the total yearly CO_2 emissions of layout L2 equal to 3.3 kt/a. Further to the right in graph 8 A, it is shown that a large part of the reduction accomplished by the heat pump is undone when a divided wall column is introduced, as the combination of both measures is infeasible. In this case, after the wall column, a membrane reactor is then applied which reduces the CO_2 emissions to a final 3.1 kt/a.

The deployment of a heat pump followed by a membrane reactor (Fig. 8B) results in a combined reduction of 3.7 kt/a in emissions from natural gas, whilst emissions from electricity generation are reduced by 0.5 kt/a to 1.7 kt/a. If this is followed by the deployment of a divided wall column an infeasible solution results after which the heat pump must be discarded whilst the membrane reactor and the divided wall column can stay. This interaction is also apparent in the second and last step of the deployment sequences of Fig. 8C and F, respectively, which implies that the divided wall column and the heat pump as designed for Layout 1 are mutually exclusive. The deployment sequences of Fig. 8d-e do not show negating of previously achieved reductions. Both sequences achieve the deepest cuts in total emissions by reducing total energy related CO_2 emissions by 2.1 kt/a, which is 58% of the expected combined CO_2 emissions reductions based on the stand-alone performance of the membrane reactor (1 kt/a), the divided wall column (1.3 kt/a) and the heat pump (1.3 kt/a), respective layouts 2, 5 and 7 in Table 2.

The CO_2 reduction potentials displayed in Fig. 8A–C and Fig. F. show that the deployment sequence significantly affects the contribution of the heat pump. Whereas Fig. 8D and E shows that for other measures the deployment sequence is of lesser importance. Though, the combined CO_2 reduction potential of the membrane reactor (1 kt/a) and the divided wall column (1,3 kt/a) is reduced to a combined CO_2 reduction of 1.5 kt/a (65%). The heat pump's CO_2 reduction is least impacted (−15%) by the deployment of the membrane reactor, as the reactor only indirectly affects the heat pump connections. The deployment sequence of the heat pump and the membrane reactor does not affect this outcome, which indicates that the deployment sequence is of lesser importance when the process change is not to the heat pump connections. The deployment sequence has a more significant impact when the process connections of the heat pump are altered by the divided wall column. The increase in the required temperature lift makes the heat pump solution infeasible. The deployment sequence does not matter in

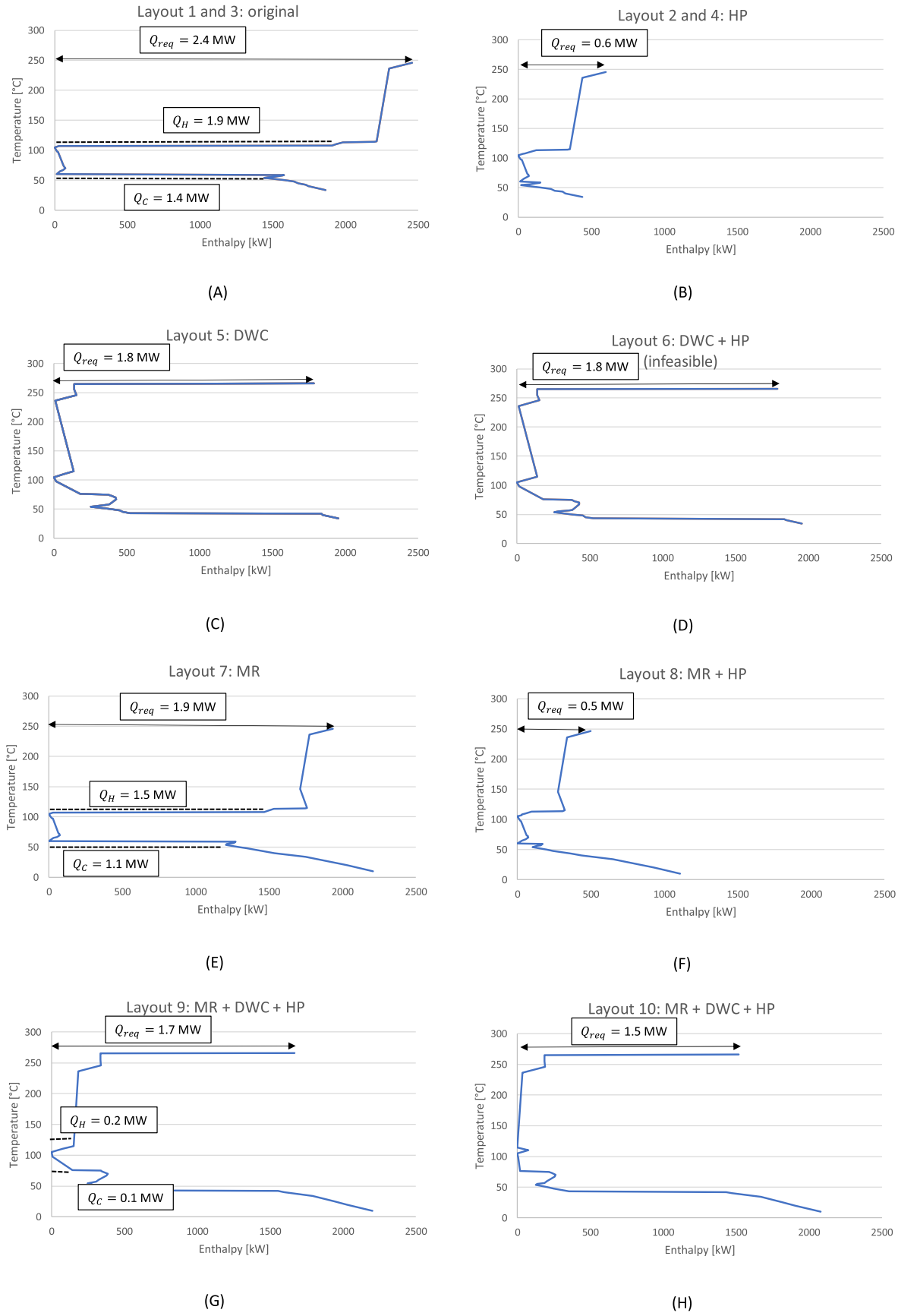

Fig. 7. Grand composite curves of the ten plausible plant layouts after the deployment of the mentioned process changes, a heat pump (HP), a divided wall column (DWC), and a membrane reactor (MR), in the order mentioned in the title of the graphs.

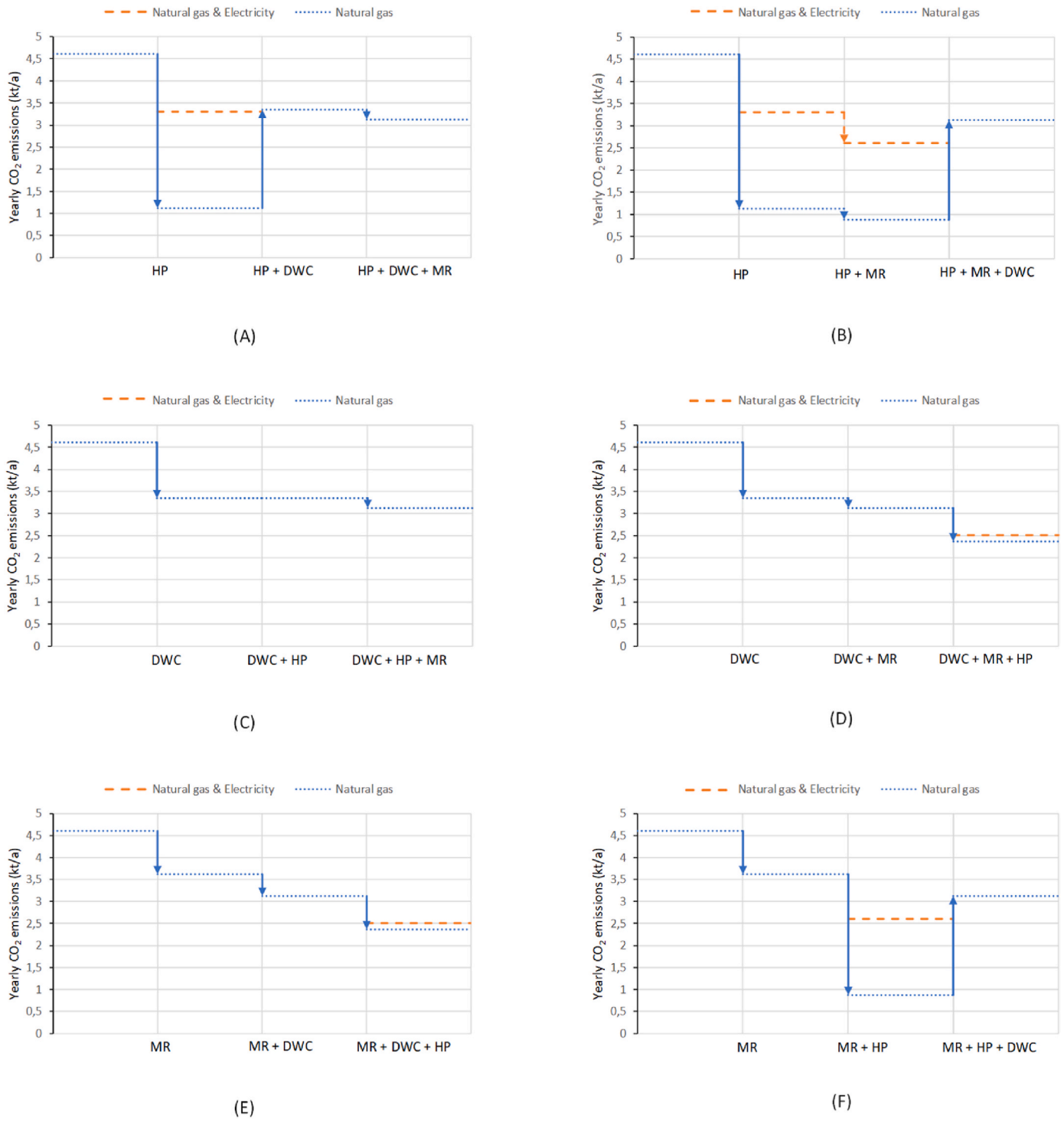

Fig. 8. Decomposition graphs of the six different deployment sequences. Changes in the amount of CO_2 emissions from natural gas combustion and electricity generation are presented in the curve. Note that not all layouts require electricity to operate and thus do not have to account for emissions from electricity generation. At each step, the process change mentioned on the x-axis is deployed, i.e., a heat pump (HP), a divided wall column (DWC), and a membrane reactor (MR).

the mutual exclusive case. The deployment sequence is of utmost importance when the heat pump, the divided wall column, and the membrane reactor are combined. Fig. 8 shows that unless the divided wall column and the membrane are deployed before the heat pump (Fig. 8D and E) an already deployed heat pump must be discarded. However, only 42% of the stand-alone CO_2 reduction potential of the three technologies will be realized. The introduction of an e-boiler did not impact the operational conditions of the other process changes, but it increased the carbon intensity of heat (i.e., kt of CO_2/MWh) and thereby increased their reduction potential.

5. Discussion

The selection and modelling of technologies is a key factor in this assessment, as a different selection of measures from Table 1 is likely to have an impact on the presented results, just as better system integration (e.g., further lowering the operating pressure in the divided wall column to lower its operational temperatures), allowing multiple heat pump

Table 2
Comparison of layouts on their heat and electricity and related CO_2 emissions. Technology none (L1) presents energy and related emissions for the reference case, and heat pump (L2) presents the energy consumption after the installment of a heat pump. The same holds for the following technology options on the list. Scope 1 savings can be calculated by comparing emissions in the fourth column. Scope 2 savings can be derived from the sixth column. – table width: 2 columns.

Technology	Heating requirements (Q_{req}) [MW]	Electricity requirements [MW]	CO_2 emissions from natural gas combustion [kt/a]	CO_2 emissions from electricity generation [kt/a]	Total energy related CO_2 emissions [kt/a]
none (L1)	2.4	0	4.6	0	4.6
heat pump (L2)	0.6	0.4	1.1	2.2	3.3
e-boiler (L3)	2.4	2.4	0	12.2	12.2
e-boiler + heat pump (L4)	0.6	0.4	0	5.1	5.1
divided wall column (L5)	1.8	0	3.3	0	3.3
divided wall column + heat pump (L6)	Infeasible solution				
membrane reactor (L7)	1.9	0	3.6	0	3.6
membrane reactor + heat pump (L8)	0.5	0.4	0.9	1.7	2.6
membrane reactor + divided wall column (L9)	1.7	0	3.1	0	3.1
membrane reactor + divided wall column + heat pump (L10)	1.5	0.0 (30 kW)	2.4	0.1	2.5

sinks and sources and technological progress (e.g., the availability of heat pumps with a higher condenser temperature which can be combined with a divided wall column) could also lead to different results. It is however important to highlight that the focus of this study was not on finding the optimal solution for the case study, but rather on exploring whether sequencing would impact the results. In this context, the selected technologies proved to be a good selection as they covered the entire range from marginal to disruptive effects and changed the heat pump connections both directly and indirectly.

The assumption that the expected carbon intensity of the Dutch electricity grid will average at 0.569 kg/kWh between 2020 and 2029 has a significant impact on the performance of an e-boiler and a heat pump and favours non-electrification measures. The performance of the heat pump and the e-boiler drastically increases with the expected halving of the well-to-wheel CO_2 emissions in 2030. The total energy-related CO_2 emissions from a sole heat pump would then reduce to 2.2 kt/a, which is 0.3 kt/a less than the current best option at 2.4 kt/a. The combination of the heat pump with the membrane reactor would be the best option in this future scenario with net yearly emissions of 1.8 kt.

The different levels of interactions have implications for the usability of sequencing tools, like a MACC. Even with the weakest interactions, those between the divided wall column and the membrane reactor, very conservative estimates are required to provide a good enough basis for the deployment of changes to the reaction and separation section, as only 65% of the stand-alone CO_2 emission savings were realized when the membrane reactor (1 kt/a) was combined with the divided wall column (1.3 kt/a) and a total savings of 1.5 kt/a was realized. Changes in the power section will have a similar impact and scale the savings of other technologies with the ratio of the new carbon-intensity to the previous carbon-intensity of the energy carrier. Stronger interactions were found between the waste heat recovery section and the separation section, where the heat pump was connected to the distillation column that was replaced by the divided wall column. The mutual exclusivity of these measures, based on the technically impossible heat delivery temperature of the heat pump, resulted in the nullifying of the heat pump's savings potential.

6. Conclusions and recommendations

This study aimed to show how the deployment sequence of CO_2 mitigation measures affects their combined CO_2 reduction potential. The results of the case study show that the deployment sequence severely impacts the combined CO_2 reduction potential when heat integration measures are considered with other heat-related process changes. Especially when changes to the process connections of the heat integration measures are considered. The deployment sequence of process changes in the reaction and separation section did not affect their combined CO_2 reduction potential.

Detrimental effects on the combined CO_2 reduction potential were found for process changes in the reaction, separation, and waste heat recovery section. The impact of these effects ranged from a significant reduction that could be overcome with conservative estimates when combining technologies in the reaction and separation section (−35%) to a technology lock-in that hindered further decarbonization when considering heat integration measures.

Decarbonizing heat sources with an e-boiler did not affect the energy and mass balance and therefore not the heat integration potential of the production plant. From a technical point of view this technology should be deployed last to avoid over dimensioning. The e-boiler did change the CO_2 reduction potential of the other measures, as it increased the carbon-intensity of the heat sources.

Not considering the impact of the deployment sequence on the combined CO_2 reduction potential of mitigation measures can have a significant impact. This was demonstrated by the mutual exclusivity of the heat pump and the divided wall column and the formation of new heat pump opportunities by deploying a membrane reactor together with a divided wall column. Sequencing approaches, like the MACC, must take these interactions into account and be careful when combining measures. A MACC should only be applied under very stringent conditions and exceptions and always consider the possibility of detrimental effects. Conservative estimates may be enough when combining process changes in the reaction and separation section, but new methods need to be developed for the combined assessment with process changes to the waste heat recovery section, especially when changes to the process connections of the waste heat technology are considered.

Credit author statement

B.W. (Brendon) de Raad, Conceptualization, Project admin, Software, Validation, Visualization, M. (Marit) van Lieshout, Conceptualization, Resources, Supervision, Editing, Reviewing, (Lydia) Stougie, Conceptualization, Resources, Supervision, Editing, Reviewing, Andrea (C.A.) Ramirez Ramirez, Conceptualization, Resources, Supervision, Editing, Reviewing.

Declaration of competing interest

The authors declare that they have no known competing financial interests or personal relationships that could have appeared to influence the work reported in this paper.

Data availability

The authors do not have permission to share data.

Acknowledgments

The authors would like to thank the students of the specialization in *Process technology & Energy transition* at the Rotterdam University of Applied Science for their critical questions and assistance with the data collection.

References

[1] Xia F, et al. Identification of key industries of industrial sector with energy-related CO2 emissions and analysis of their potential for energy conservation and emission reduction in Xinjiang, China, vol. 708. Science of the total environment; 2020, 134587.
[2] Åhman M, Nilsson LJ. Decarbonizing industry in the EU: climate, trade and industrial policy strategies. In: Decarbonization in the European union. Springer; 2015. p. 92–114.
[3] Yáñez E, et al. Unravelling the potential of energy efficiency in the Colombian oil industry. J Clean Prod 2018;176:604–28.
[4] Hasanbeigi A, et al. Energy efficiency improvement and CO2 emission reduction opportunities in the cement industry in China. Energy Pol 2013;57:287–97.
[5] Nwachukwu CM, Wang C, Wetterlund E. Exploring the role of forest biomass in abating fossil CO2 emissions in the iron and steel industry–The case of Sweden. Appl Energy 2021;288:116558.
[6] Johansson D, et al. Assessment of strategies for CO2 abatement in the European petroleum refining industry. Energy 2012;42(1):375–86.
[7] Lambauer J, et al. Large-capacity industrial heat pumps. Potential, obstacles, examples; Gross-Waermepumpen in der Industrie. Potenziale, Hemmnisse und Musterbeispiele. Die Kaelte-und Klimatechnik; 2008. p. 61.
[8] Bühler F, et al. Evaluation of energy saving potentials, costs and uncertainties in the chemical industry in Germany. Appl Energy 2018;228:2037–49.
[9] Yáñez E, et al. Exploring the potential of carbon capture and storage-enhanced oil recovery as a mitigation strategy in the Colombian oil industry. Int J Greenh Gas Control 2020;94:102938.
[10] McKinsey. Pathways to a low-carbon economy: version 2 of the global greenhouse gas abatement cost curve. 2010.
[11] Vogt-Schilb A, Hallegatte S. Marginal abatement cost curves and the optimal timing of mitigation measures. Energy Pol 2014;66:645–53.
[12] Ekins P, Kesicki F, Smith AZ. Marginal abatement cost curves: a call for caution. University College London; 2011.
[13] Berghout N, et al. Assessing deployment pathways for greenhouse gas emissions reductions in an industrial plant–A case study for a complex oil refinery. Appl Energy 2019;236:354–78.
[14] Wiertzema H, Svensson E, Harvey S. Bottom–up assessment framework for electrification options in energy-intensive process industries. Front Energy Res 2020;8:192.
[15] IEA. Energy efficiency 2019. IEA; 2019.
[16] Marina A, et al. An estimation of the European industrial heat pump market potential. Renew Sustain Energy Rev 2021;139:110545.
[17] Brückner S, et al. Industrial waste heat recovery technologies: an economic analysis of heat transformation technologies. Appl Energy 2015;151:157–67.
[18] Løken PA. Process integration of heat pumps. J Heat Recovery Syst 1985;5(1):39–49.
[19] Douglas MJ. Conceptual design of chemical processes. McGrawHill; 1988.
[20] Townsend D, Linnhoff B. Heat and power networks in process design. Part I: criteria for placement of heat engines and heat pumps in process networks. AIChE J 1983;29(5):742–8.
[21] Townsend D, Linnhoff B. Heat and power networks in process design. Part II: design procedure for equipment selection and process matching. AIChE J 1983;29(5):748–71.
[22] Kemp IC. Pinch analysis and process integration: a user guide on process integration for the efficient use of energy. Elsevier; 2011.
[23] March L. Introduction to pinch technology. Targeting House; 1998. Gadbrook Park, Northwich, Cheshire, CW9 7UZ, England.
[24] Gallego L. release 0.4.6. accessed on 29 Dec. 2021. PinchAnalysis-Console 2019. https://github.com/LuisEduardoCorreaGallego/PinchAnalysis-Console.
[25] Olsen D, et al. Integration of heat pumps in industrial processes with pinch analysis. In: 12th IEA heat pump conference; 2017.
[26] Oluleye G, et al. Evaluating the potential of process sites for waste heat recovery. Appl Energy 2016;161:627–46.
[27] Van de Bor D, Ferreira CI. Quick selection of industrial heat pump types including the impact of thermodynamic losses. Energy 2013;53:312–22.
[28] Zijlema P. Berekening van de standaard CO2-emissiefactor aardgas t.b.v. nationale monitoring 2020 en emissiehandel 2020. RVO; 2019.
[29] Vakkilainen EK. Steam generation from biomass: construction and design of large boilers. Butterworth-Heinemann; 2016.
[30] Abels-van Overveld M, et al. Klimaat-en energieverkenning 2019. 2019.
[31] Van Gerpen J. Biodiesel processing and production. Fuel Process Technol 2005;86(10):1097–107.
[32] Luna D, et al. Technological challenges for the production of biodiesel in arid lands. J Arid Environ 2014;102:127–38.
[33] Construction AL-E. Lurgi MegaMethanol(tm). 2021.
[34] Ma F, Hanna MA. Biodiesel production: a review. Bioresour Technol 1999;70(1):1–15.
[35] Abdullah SHYS, et al. A review of biomass-derived heterogeneous catalyst for a sustainable biodiesel production. Renew Sustain Energy Rev 2017;70:1040–51.
[36] Atadashi I, Aroua M, Aziz AA. Biodiesel separation and purification: a review. Renew Energy 2011;36(2):437–43.
[37] Atadashi I, et al. The effects of catalysts in biodiesel production: a review. J Ind Eng Chem 2013;19(1):14–26.
[38] Oh PP, et al. A review on conventional technologies and emerging process intensification (PI) methods for biodiesel production. Renew Sustain Energy Rev 2012;16(7):5131–45.
[39] Soriano Jr NU, Venditti R, Argyropoulos DS. Biodiesel synthesis via homogeneous Lewis acid-catalyzed transesterification. Fuel 2009;88(3):560–5.
[40] Roschat W, et al. Biodiesel production from palm oil using hydrated lime-derived CaO as a low-cost basic heterogeneous catalyst. Energy Convers Manag 2016;108:459–67.
[41] Gupta J, Agarwal M, Dalai A. An overview on the recent advancements of sustainable heterogeneous catalysts and prominent continuous reactor for biodiesel production. J Ind Eng Chem 2020.
[42] Cao P, Dubé MA, Tremblay AY. Methanol recycling in the production of biodiesel in a membrane reactor. Fuel 2008;87(6):825–33.
[43] Dubé M, Tremblay A, Liu J. Biodiesel production using a membrane reactor. Bioresour Technol 2007;98(3):639–47.
[44] Atkinson S. Making large-scale reactions more energy efficient. 2021. MA Business London.
[45] Saleh J, Tremblay AY, Dubé MA. Glycerol removal from biodiesel using membrane separation technology. Fuel 2010;89(9):2260–6.
[46] Atadashi I, et al. Refining technologies for the purification of crude biodiesel. Appl Energy 2011;88(12):4239–51.
[47] Bateni H, Saraeian A, Able C. A comprehensive review on biodiesel purification and upgrading. Biofuel Res J 2017;4(3):668–90.
[48] Gomes MCS, Pereira NC, de Barros STD. Separation of biodiesel and glycerol using ceramic membranes. J Membr Sci 2010;352(1–2):271–6.
[49] He H, Guo X, Zhu S. Comparison of membrane extraction with traditional extraction methods for biodiesel production. J Am Oil Chem Soc 2006;83(5):457–60.
[50] Savaliya ML, Dhorajiya BD, Dholakiya BZ. Current trends in separation and purification of fatty acid methyl ester. Separ Purif Rev 2015;44(1):28–40.
[51] Kiss A, et al. Innovative biodiesel production in a reactive dividing-wall column. In: Computer aided chemical engineering. Elsevier; 2012. p. 522–6.
[52] Kiss AA, Bildea CS. A review of biodiesel production by integrated reactive separation technologies. J Chem Technol Biotechnol 2012;87(7):861–79.
[53] Kiss AA, Ignat RM. Enhanced methanol recovery and glycerol separation in biodiesel production–DWC makes it happen. Appl Energy 2012;99:146–53.
[54] IEA I. Energy technology perspectives 2017. Catalysing Energy Technology Transformations; 2017.
[55] Rubin E, De Coninck H. IPCC special report on carbon dioxide capture and storagevol. 2; 2005. p. 14. UK: Cambridge University Press. TNO (2004): Cost Curves for CO2 Storage, Part.
[56] Marsidi M. Electric industrial boiler - technology factsheet (TNO). 2018.
[57] Klarenbeek D. Personal communications. 2020.
[58] Arpagaus C, et al. High temperature heat pumps: market overview, state of the art, research status, refrigerants, and application potentials. Energy 2018;152:985–1010.
[59] Mateu-Royo C, et al. Advanced high temperature heat pump configurations using low GWP refrigerants for industrial waste heat recovery: a comprehensive study. Energy Convers Manag 2021;229:113752.
[60] Schlosser F, et al. Large-scale heat pumps: applications, performance, economic feasibility and industrial integration. Renew Sustain Energy Rev 2020;133:110219.